Atmósfera 37, 209-232 (2023)
https://doi.org/10.20937/ATM.53039

The planetary boundary layer physical processes, the secondary thermal baroclinic circulation and inertial oscillation contribution to diurnal variation of the Etesian winds over the Aegean Sea

Nicholas G. PREZERAKOS

Emeritus Professor, School of Engineering, University of West Attica, Ancient Eleonas University Campus, Egaleo, 122 41, Attica, Greece; Honorary President of the Hellenic (Greek) Meteorological Society.
Correspondence: npreze@uniwa.gr

Received: February 23, 2021; accepted: May 6, 2022

RESUMEN

Los vientos etesianos constituyen un fenómeno climatológico importante, que no sólo modera el calor durante el verano en el mar Egeo, sino que también proporciona una fuente de energía renovable limpia. A pesar de que varios artículos han intentado explicar sus características dinámicas y físicas, los procesos respectivos que impulsan la variación diurna de la velocidad del viento no se entienden completamente. El objetivo de este trabajo es identificar los procesos responsables de la variación diurna con la velocidad máxima del viento observada alrededor del mediodía y la mínima alrededor de la medianoche. Las soluciones analíticas de una ecuación primitiva establecida en forma euleriana, después de introducir condiciones y aproximaciones adecuadas, revelan una oscilación inercial sobre el mar Egeo. Los datos basados en observaciones directas, los análisis de alta resolución ECMWF IFS y las simulaciones de alta resolución con el modelo Investigación y Pronóstico del Clima (WRF, por sus siglas en inglés) se utilizan para averiguar el tipo y la estructura de la capa límite planetaria (PBL) sobre el mar Egeo. Esta PBL parece ser de carácter marino y turbulento, principalmente durante el día y menos durante la noche. Se ha encontrado que el impacto directo de las circulaciones locales y regionales impulsadas térmicamente es la causa principal de la variación diurna del viento observado y en parte de la oscilación inercial. Los resultados de las simulaciones numéricas certifican estos hallazgos. Además, el momento y los intercambios de calentamiento newtonianos por los procesos físicos dentro de la PBL, donde está presente el viento de gradiente junto con escalas más pequeñas de movimientos atmosféricos, también son necesarios para explicar la variabilidad de los vientos etesianos.

ABSTRACT

Etesian winds constitute an important climatological phenomenon, which does not only moderate the heat during the summer in the Aegean Sea, but provides a source of clean renewable energy as well. Even though several papers have attempted to explain their dynamical and physical characteristics, the respective processes that drive the diurnal variation of the wind speed are not fully understood. The objective of this paper is to identify the processes responsible for diurnal variation with observed maximum wind speed around noon and minimum around midnight. Analytical solutions of a primitive equation set in Eulerian form, after introducing suitable conditions and approximations, reveal an inertial oscillation over the Aegean Sea. Data based on direct observations, ECMWF IFS high resolution analyses and high-resolution simulations with the Weather Research and Forecasting (WRF) model are utilized to find out the type and structure of the planetary boundary layer (PBL) over the Aegean Sea. This PBL appears to be of a marine character and turbulent mostly during the day but less during the night. The direct impact of local and regional thermally-driven circulations is found to be the main cause of the diurnal variation of the observed wind and partly the inertial oscillation. Results from numerical simulations certify these findings. Furthermore, the momentum and Newtonian heating exchanges by the physical processes inside the PBL, where the gradient wind together with smaller scales of atmospheric motions exist, are also necessary for explaining the variability of the Etesian winds.

Keywords: planetary boundary layer structure, Eulerian equations of inertial oscillation, planetary boundary layer momentum moisture and heat transfer, local and regional sea and mountain breezes, high resolution analyses and simulations.

1. Introduction

"Etesians" are seasonal winds which blow over the Aegean Sea (Fig. 1) during the warm season of the year, mainly in July and August. These winds, which exhibit a distinct diurnal variation, are an important moderator of the summer heat in the southeastern Mediterranean region and additionally provide a significant source of renewable energy. Although Etesians have been studied satisfactorily (Carapiperis 1955, 1968, 1970; Constantakopoulos, 1959; Metaxas, 1970; Prezerakos, 1975), the physical mechanisms responsible for the diurnal variation of their speed is still debated.

Fig. 1. Locations and geographical features mentioned in the text. Red cross spots: grid points close to Limnos, Naxos and Heraklion (from north to south). Long thick arrows: direction of regional baroclinic circulation. Short thin arrows: local sea breeze direction.

The atmospheric circulation consists of a variety of interacting scales of motion ranging through the microscale, mesoscale, synoptic-scale and global scale. Although these scales cannot be adequately resolved by dynamical and parametrized physical processes, the use of mathematical-statistical methods (e.g., the complex empirical orthogonal function [CEOF]) (Dafka et al., 2018; Cahuich-López et al., 2020) have proven to be very efficient tools to discriminate the influence of each scale of motion in the resultant atmospheric circulation. There are many studies in the international meteorological literature dealing with the thermally driven circulation inside the planetary boundary layer (PBL) supporting the view that the interaction between synoptic-scale barometric gradient wind and sea-land breezes is an ordinary physical phenomenon. Most of these studies are cited in Cahuich-lópez et al. (2020), Arrillaga (2020) and the earlier ones in Prezerakos (1986). Therefore, the sea breeze, being a local to regional scale atmospheric circulation, must affect the Etesian winds and, in addition, micro-scale sub grid physical processes such as orographic drag and thermal and mechanical turbulence affect mostly the land-sea circulation (Arrillagar, 2020). These hypotheses remain to be studied quantitatively.

Tyrlis and Lelieveld (2013) investigated Etesian winds through the spectrum of the atmospheric motion, complementing the classical one by Repapis et al. (1977), and showed that almost every scale of this spectrum contributes to the genesis and maintenance of Etesian winds. It also supports the impact of the local and regional thermal baroclinic circulation upon Etesian winds. However, studies focusing on the diurnal variation of the Etesian winds over the Aegean Sea have not yet been conducted.

1.1 The concept of type A Etesian winds

Numerous papers cited in Prezerakos (2022) provide a detailed description of the Aegean climate during the warm season, the background atmospheric circulation and the physical characteristics of Etesian winds. Prezerakos (2022) provides a set of objective criteria to classify the Etesian winds in three distinct types (A, B, C), giving their starting dates.

A spell of fresh Etesian winds, called outbreak by Tyrlis and Lelieveld (2013), occurs when a surface anticyclone arrives over the Balkans behind a cold front. This synoptic situation is exclusively responsible for the configuration of the frequency of

appearance of the Etesian winds outbreaks and therefor closely associated with the frequency of the Rossby synoptic-scale waves. This finding in Prezerakos (2022) is in agreement with those of Metaxas and Bartzokas (1994), who demonstrated that the mean sea level pressure (MSLP) activity center driving the variability of the Etesian winds is positioned over the Northwest Balkans. With the appearance of an Etesian winds outbreak, significant increase of wind intensity usually occurs without any diurnal variability being observed for a minimum of one and maximum of seven consecutive days. These intensified Etesian winds with no diurnal variation are the so-called type B or Etesian winds outbursts studied in Prezerakos (2022). Thereafter, the wind intensity displays a gradual decrease from day to day and at the same times a distinct diurnal variation typically about 7.5 m/s at noon falling to less than 5 m/s at midnight. These winds are referred to as Etesian winds type A (Andreakos et al., 1984). When wind speed weakens during the day, the sea breeze prevails. This is clearly seen at meteorological stations, where the sea breeze has the opposite direction to the Etesian winds (e.g., Hellinikon, WMO 16716) close to Athens and at the coasts of northern Greece. The days when the sea breeze prevails at Hellinikon are referred to as Etesian winds type C (Carapiperis, 1968; Andreakos et al., 1984).

1.2 Goals of this study

The main goal of this paper is to study only the dynamics and physics of the diurnal variation of type A Etesian winds, which is still a matter of debate. To address this main goal, almost all the topics associated with the variability of the Etesian winds have been considered, namely: the physical geography of Greece (especially the orography and the land-sea distribution), the structure of the PBL with its wind shear, and the mechanical and thermal turbulence resulting in vertical advection of momentum and Newtonian heating. Furthermore, an attempt is made to explore the genesis and behavior of the sea-land breeze in the region under study and the way in which it influences the Etesian winds. Finally, an investigation is made to verify if the inertial oscillation (IO) concept (Blackadar, 1957; van de Wiel et al., 2010) applies and contributes to the Etesian wind diurnal variation.

This article is structured as follows: section 2 describes the data and the methodology utilized, with subsections 2.1 Data, 2.2 Methodology, 2.2.2 Theoretical identification of the physical factors contributing to the Eulerian variability of the type A Etesian winds. Section 3 presents the results derived from the processing of the data of this study and a further discussion on these results follows in subsections 3.1 The PBL structure over the Aegean Sea during Etesian winds season, 3.2 Possible inertial oscillation in the Aegean Sea in summer, 3.3 Local and regional secondary baroclinic circulation and its contribution, 3.4 A numerical experiment verifying the conceptual aspects. Finally, section 4 presents conclusions and suggestions for future relevant works.

2. Data and methodology

2.1. Data

The data utilized in this study were provided by:

a. The Hellenic National Meteorological Service (HNMS). These are original meteorological observations from June to September 1975-2015 of the international synoptic stations, namely Limnos, Naxos, Iraklion, and Hellinikon, with WMO code numbers 16650, 16732, 16754, and 16716, respectively.
b. The European Center of Medium-Range Weather Forecasts (ECMWF) gridded output from Interim and the operational model at 9-km resolution.
c. The National Center of Atmospheric Research (NCAR) NCEP-GFS gridded output at 27-km resolution.

This dataset was utilized as follows:

a. To identify the dates of Etesian winds type A and C via Excel and Visual Basic, bearing in mind their definitions mentioned in section 1.1.
b. To investigate the nature and type of the PBL over the Aegean Sea.
c. For the execution of the 2020 numerical experiment.

Figure 2 was drawn with Excel and Figures 1, 3, 4, 5, 7 with Mathematica. The colored Figures 8 to 14 and the Mean SkewT-logp diagrams of Figure 3 are visualized outputs of WRF-ARF. Figure 6 was provided by the HNMS web page.

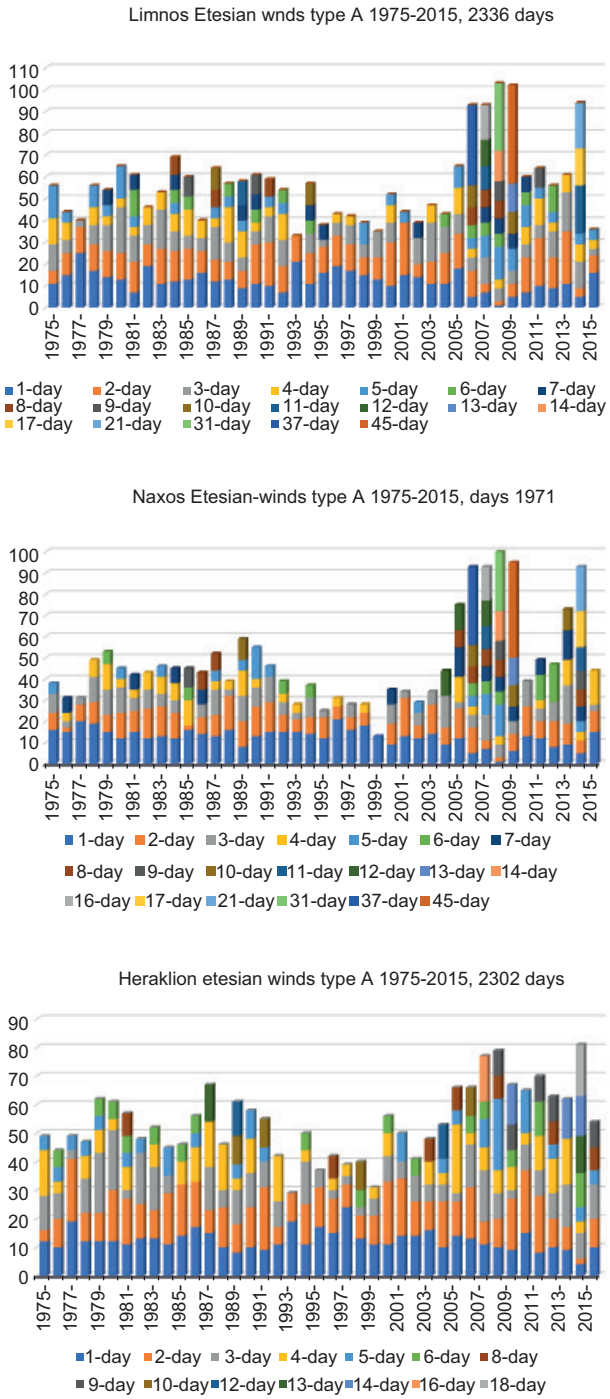

Fig. 2. Frequency of occurrence (number per year) and duration (days) of Etesian winds type A spells (colors) for the period 1975-2015 in Limnos, Naxos and Iraklion meteorological stations.

2.2 Methodology

2.2.1. Definitions of frequency, dates and duration of Etesian winds type A and C

Firstly, we utilized the real-time data to determine the dates during which Etesian winds type A and C are blowing in June, July, August, and September from 1975 to 2015. For this to be accomplished, we subtracted the dates of Etesian winds type B detected and selected in Prezerakos (2022) from the original record of the Etesian winds for the whole number of dates in the time period considered. The deriving number is the sum of type A and C dates. Secondly, we applied the objective criterion set by Carapiperis (1968) on the real-time data, to identify C dates at the WMO 16716 station. This criterion is: "When, during Etesian winds season the wind at the 12:00 UTC observation of a day, at Hellinikon station (WMO 16716) gets a direction of the sector 160º- 240º, then this day belongs to Etesian winds Type C". Thus, we detected and selected the dates on which, at a certain place, the sea breeze and the Etesian winds occur with opposite directions and the sea breeze prevails. These dates constitute the number of days, a total of 1854, when the Etesian winds type C were occurring over the Greek seas.

The frequency of appearance of Etesian winds type A per year and the number of consecutive days is illustrated in Figure 2. The colors denote the number of consecutive days of various Etesian winds type A at the main synoptic (international) meteorological stations Limnos, Naxos and Iraklion. The most impressive element of this figure is that during the years 2006-2009 and 2014 there were 21, 31, 27, and 45 consecutive-date spells in Limnos and Naxos, and up to 18 in Iraklion. Etesian winds observations of the period 1975-2015 at these three meteorological stations are completely classified in types A, B and C; moreover, 22 dates at Limnos, 304 in Naxos and 224 at Iraklion, which although belong to type C, do not show the diurnal variation of the wind according to the induced definition, that is, they belong to type B, and would be subtracted from 1854 dates of each station to be studied separately. In addition, the dates of Etesian winds type C include the rare cases where the gradient wind blows over the Aegean Sea from the south sector, thus it is very easy to be selected and studied. All these data are available by the author

2.2.2. Theoretical identification of physical factors possibly contributing to the Eulerian variability of type A Etesian winds

Dealing with the wind inside the PBL we ordinarily consider the Ekman's equations assuming balance between pressure gradient, Coriolis and friction forces (Stull, 1988) in Eulerian form, thus masking the process to arrive at this form from primitive equations based on Newton's second low. For the readers' convenience, here we repeat all the steps needed to transform the equations from their Lagrangian format to Eulerian one. So the physical factors contribute to the observed wind variability will be better revealed. The equations of the horizontal atmospheric motion in a Cartesian reference system moving with the Earth, with height (z) as vertical coordinate, after a few approximations (Wiin-Nielsen, 1974) are:

$$\begin{aligned}\frac{du}{dt} &= fv - \frac{1}{\rho}\frac{\partial p}{\partial x} + \frac{1}{\rho}F_{\mathrm{x}} \\ \frac{dv}{dt} &= -fu - \frac{1}{\rho}\frac{\partial p}{\partial y} + \frac{1}{\rho}F_{\mathrm{y}}\end{aligned} \tag{1}$$

where (u, v, w) are the components of actual wind, f is the Coriolis parameter, ρ the air density, p the mean sea level pressure and (F_{x}, F_{y}) the friction force components, which include all the physical processes near surface. For a turbulent or/and convective boundary layer, Arya (1985) pointed out that in a rotating frame of reference, the friction force on a fluid element may not be parallel and opposite to the velocity vector, as it happens on the surface and top of the PBL, suggesting a more realistic balance of pressure gradient, Coriolis and friction. Thus, setting frictional forces inside the PBL to $\frac{1}{\rho}F_x = K\frac{\partial^2 u}{\partial z^2}$, $\frac{1}{\rho}F_x = K\frac{\partial^2 u}{\partial z^2}$, K is the eddy diffusivity. Eq. (1) becomes:

$$\begin{aligned}&\frac{\partial u}{\partial t} + u\frac{\partial u}{\partial x} + v\frac{\partial u}{\partial y} + w\frac{\partial u}{\partial z} = \\ &fv - \frac{1}{\rho}\frac{\partial p}{\partial x} + \frac{1}{\rho}F_{\mathrm{x}}, \\ &\frac{\partial v}{\partial t} + u\frac{\partial v}{\partial x} + v\frac{\partial v}{\partial y} + w\frac{\partial v}{\partial z} = \\ &-fu - \frac{1}{\rho}\frac{\partial p}{\partial y} + \frac{1}{\rho}F_{\mathrm{y}}\end{aligned} \tag{2}$$

From Eq. (2), we can see that the local time variability of the actual wind depends on many factors, most of which are non-linear, e.g., the terms of advection, especially inside the turbulent PBL. These non-linear terms are responsible for the interaction of the various scales of atmospheric motion leading to the well-known "cascade process" (Holton and Hakim, 2013; Wiin-Nielsen, 1973).

Many researchers usually divide the actual wind in two components: geostrophic and ageostrophic, and consider the partial derivative with respect to time of the geostrophic component constant, e.g.,

$$\begin{aligned}&\mathbf{V} = \mathbf{V}g + \mathbf{V}a \rightarrow \mathbf{V} = \mathbf{V}_g + \frac{1}{f}\left[\mathbf{k}\times\frac{d\mathbf{V}_a}{dt} + \mathbf{k}\times\right. \\ &\left.\frac{\partial \mathbf{V}_g}{\partial t} + V\,\mathbf{k}\times\frac{\partial \mathbf{V}_g}{\partial s} + w\mathbf{k}\times\frac{\partial \mathbf{V}_g}{\partial z} - \mathbf{k}\times\mathbf{F}_f\right]\end{aligned} \tag{3}$$

As seen in Eq. (3), the ageostrophic component $\mathbf{V}_{\mathrm{a}}$ has been expressed as five terms (Prezerakos, 1985; Prezerakos and Flocas, 2002), interpreted as follows:

1. Acceleration of ageostrophic wind, which cannot be resolved further.
2. Isallobaric term, which represents the isallobaric wind due to changes of the pressure tendencies.
3. Downwind changes in the pressure gradient (confluence, difluence).
4. Vertical exchange of momentum.
5. Any kind of friction, mainly in the boundary layer.

Eq. (3) shows clearly in vector form all the physical factors the observed wind depends on, being almost the same with those of Eq. (2). Although none of these factors is constant in case of the Etesian winds of type A, at a fixed Eulerian grid point the first three terms, although very important in case of Etesian winds type B (Prezerakos, 2022), can be considered zero for the sake of simplicity. However, the last two terms could be proved significant, as we shall see below. When a type A Etesian wind occurs over the Aegean Sea, the geostrophic wind is almost clearly constant at least between three hourly synoptic observations and thus the synoptic-scale pressure gradient, which governs it. Consequently, for a better physical explanation of the phenomenon, our interest focuses on the diurnal

variation of the geostrophic departure (ageostrophic wind). It is this part of the wind, which includes all the varying components of the atmospheric spectrum of motion being created by processes belonging to smaller scales, namely, orography, distribution of sea-land, PBL state including sub grid mountain drag, vertical exchange of momentum and heat by mechanical and thermal turbulence, surface friction and the possible inertial oscillation is attributed.

After the above assumptions, Eq. (2) becomes

$$\frac{\partial u}{\partial t} = fv - \frac{1}{\rho}\frac{\partial p}{\partial x} - [w\frac{\partial u}{\partial z} - \frac{1}{\rho}F_x]$$
$$\frac{\partial v}{\partial t} = -fu - \frac{1}{\rho}\frac{\partial p}{\partial y} - [w\frac{\partial v}{\partial z} - \frac{1}{\rho}F_y] \quad (4)$$

3. Results and discussion

3.1. PBL structure over the Aegean Sea during Etesian winds season and its contribution

The actual wind observed at meteorological stations at 10 m is inside the Prandtl-layer extended in a height of 20 to 60 m just above the few centimeters depth laminar layer, and thus depends mostly on the PBL's natural characteristics and processes, especially earth surface friction and thermal and mechanical turbulence (Wiin-Nielsen, 1973). Research work based on real-time observations relative to PBL on Aegean Sea was rare before 1990. To the author's knowledge, only Mariolopoulos et al. (1981) dealt with the static state of the PBL during daytime in summer at most of the western part of the Aegean Sea, and so influenced strongly by the large land mass of Greece. They concluded that the PBL over this part of the Aegean Sea presents the ordinary unstable state over land in daytime induring summer, but, of course, influenced mostly by the marine air and, in few times, long distance inland.

Since 1990, many attempts have been made by Greek scientists to explore the PBL mainly in rural and coastal places in conjunction with atmospheric pollution and the contribution of local and regional sea-land breezes. All of these papers, which appeared in the international literature, deal with the PBL structure and their findings are mostly derived from experimental real observational data (Asimakopoulos et al., 1993; Soilemes et al., 1993; Asimakopoulos and Helmis, 1994; Helmis et al., 1995, 2002; Founda et al., 1997; Tombrou et al., 2007, 2015; Kostopoulos and Helmis, 2014; Dandou et al., 2017; Agathangelidis et al., 2020; Methymaki et al., 2020). The distinguished observational campaign held over the Aegean Sea (GAME) during late August and early September in 2011 (Tombrou et al., 2015; Dandou et al., 2017) provided many scientists with the necessary measurements to elaborate extensive research work relevant to the Aegean Sea PBL. However, the whole matter needs more in-depth study.

The author had stated (Prezerakos, 1975), without any supporting data, that the Aegean Sea daytime PBL resembles the corresponding one over land, because of the morphology of its surface terrain. However, after the appearance of the above-mentioned publications, a need arises for altering this conceptual aspect. Lacking the necessary real-time observations, we decided that the best alternate way to explore the structure of the PBL over the Aegean Sea was to utilize the analyses of ECMWF IFS HRES. These analyses have a horizontal space resolution 9 km and a vertical one about 137 σ levels with the four lowest at 10, 31, 54, 79 m above ground and 20 more up to 1500 m. The real data coming from the synoptic and not only ground and satellite-based observations in a time window of 6 h before and 3 h after the time of the main analyses (00:00 and 12:00 UTC), to be used as initial values, have to be subjected a treatment via the 4D-Var data assimilation technique. The 4D-Var analysis uses the IFS dynamics and physics to create a sequence of states that fits as closely as possible to the available observations. These states are consistent with the dynamics and physics of the atmosphere, as expressed by the equations of the IFS model, but do not represent explicitly the real initial state of each particle in the atmosphere being at best a smoother motion on a relatively large scale (Owens and Hewson, 2018). Observations of wind speed and direction from ships and buoys are used by the IFS data assimilation system, but not those from land stations or even from islands. Thereafter, the IFS analyses being transferred to a meso-scale nested model as initial and lateral boundary values must be completed with all the available observations, by the receiver model's own data assimilation system, especially the winds from islands and coastal stations (Owens and Hewson, 2018).

In order to better detect the structure of the PBL over the Aegean Sea, the above-mentioned procedure was applied. Thus, we selected the ECMWF IFS HRES analyses for the Greek territory during the middle of the Etesian winds season (20 to 31 July 2020) at 00:00 and 12:00 UTC to feed the mesoscale model WRF-ARW v.4.0, having a horizontal space resolution of 1.8 km in the innermost nest. Although we have already cited many sources existing in the WRF documentation, it is useful to mention the selected PBL schemes because of the optional character of the model. These are the Dudhia scheme (Dudhia, 1989), the Rapid Radiative Transfer Model (RRTM) scheme (Mlawer et al., 1997), the WRF YSU scheme (Hong et al., 2006), the Revised MM5 similarity theory surface layer scheme (Jiménez et al., 2012) and the Monin-Obukhov similarity theory (Monin and Obukhov, 1954). This version 4.0 gets a hybrid hydrostatic-pressure vertical coordinate system (Skamarock et al., 2019; Dafis, 2020) with no convective parameterization and the outputs are saved every 1 h. The meteorological parameters under consideration are temperature, dew point, and wind. After calculating the mean values, we depicted the results in Figure 3a, b showing the structure of the PBL over the sea at three grid points close to Limnos, Naxos and Heraklion (Fig. 1, red crosses).

We start our discussion with Naxos, which lies at the center of the Aegean Sea (Fig. 1), where during July the sea surface temperature (SST) is 22 to 24 ºC, much lower than the 2-m air temperature, especially during daytime. However, in rare cases, very few parts of the south Aegean Sea have an SST up to 27 ºC, which is slightly greater than 2-m air temperature. Figure 3a shows an internal boundary layer with weak to moderate winds and cooling from below. As the wind force gradually decreases after sunset about 17:30 UTC (20:30 LT), the relatively little mechanical turbulence influences a shallow air layer configuring it to get a constant temperature with base at surface and top at about 750 m. At that level, the maximum wind force appears to be below 700 m, revealing a low-level nocturnal jet. Figure 3a verifies the findings of many researchers, demonstrating that Etesian winds flow are relatively shallow below 700 hPa, and synoptic-scale subsidence dominates their flow as shown by the abrupt increase in the isobaric distance of bold green and red lines above the lifting condensation level (LCL). The wind profile also shows a distinct turning to the right with height, which means warm advection, thus there is a tendency for stabilization of the atmosphere above the central Aegean Sea. At the same time, close to Heraklion (not shown), where the SST is greater and the cooling from below is lower, an isothermal shallow layer forms from the surface up to 650 m. Above it there is a smooth temperature inversion with a top at 1000 m. Here it is worth noting that in the above-mentioned rare cases in the south Aegean Sea, SST is slightly greater than the 2-m air temperature, then a sensible heat flux not more than 50 W m^{-2} during the day and night occurs. This physical process is clearly shown by the outputs of the numerical experiment (see subsection 3.4). In the nocturnal low-level jet (LLJ) identified at the layer between 600 and 1000 m just south of Limnos, the SST shows its lowest value around 20 ºC and the cooling from below is stronger. So, the PBL structure resembles that at Naxos, with the nocturnal low jet appearing to be at 750-1000 m and stronger (about 14 m s^{-1}). The picture of the nocturnal PBL over the Aegean Sea, determined by real-time data utilized by Greek researchers so far (Helmis et al., 1995; Founda, et al., 1997; Tombrou et al., 2007; Dandou et al., 2017) appears to be mostly similar to this one, structured by the initial analyses of WRF.

The daytime structure of the PBL derived in this study over the Aegean Sea presents special interest since it differs from that which the author supported in the past (Prezerakos, 1975). Figure 3b shows that the cooling from below is preserved during the day, but the mechanical turbulence is stronger than during nighttime due to stronger winds. Therefore, the stable character of the lowest PBL usually ceases. This part, due to the strong turbulent mixing tends to adopt a constant potential temperature. Above it, where the mechanical turbulence is weak, a smooth temperature inversion with a top at about 1300 m appears. The maximum value of the wind force appears to be not just at the top of the inversion but inside the inversion layer, being greater than the nocturnal value, which reveals the presence of sea breeze. This turning to the left of the downward wind is due to the increase of friction. The other characteristics of the PBL are the same as those at night. The thermodynamic diagrams

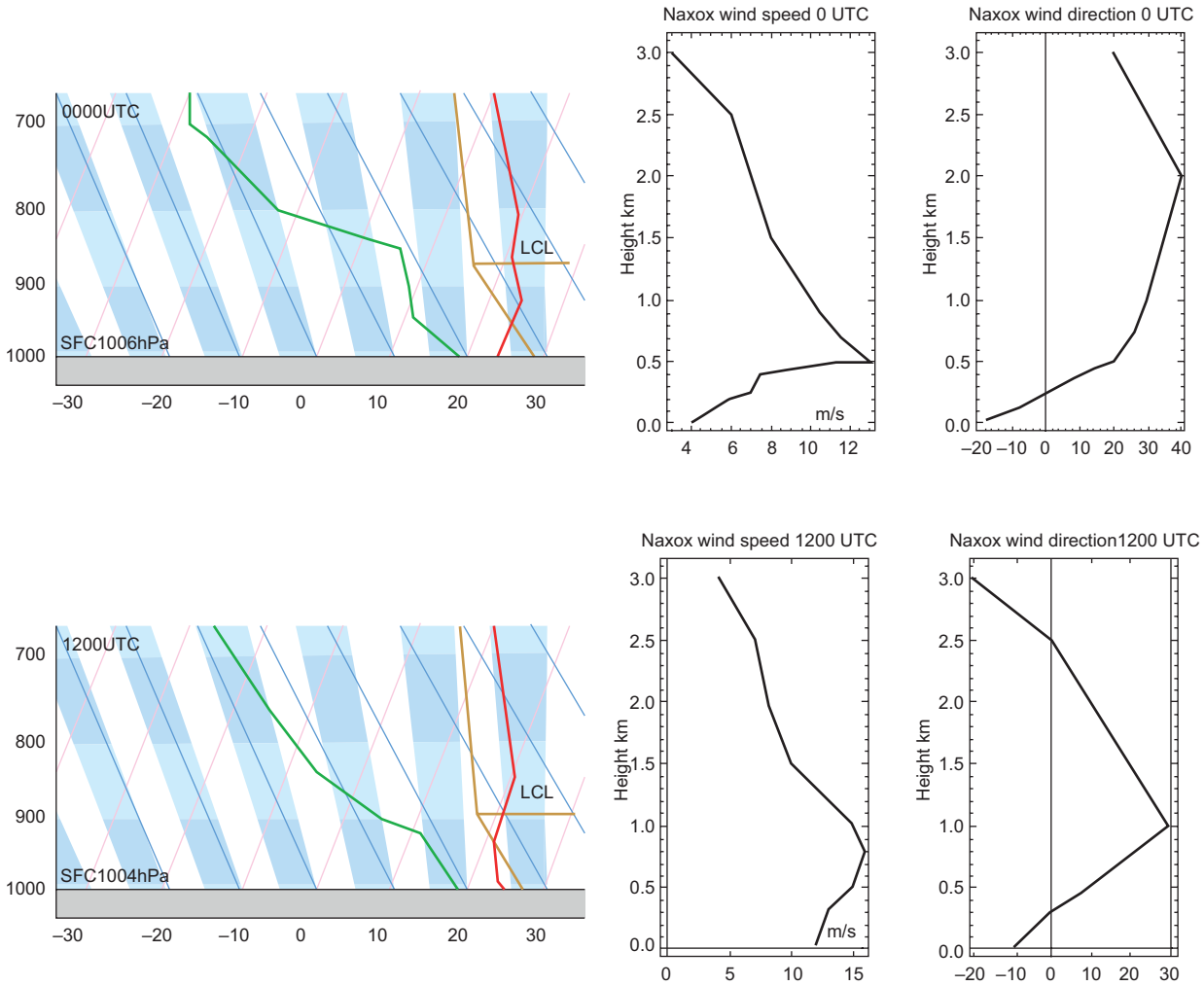

Fig. 3. Mean skewt-logp diagram, red bold line and wind profiles of Naxos from July 21 to 31, 2020 at (a) 00:00 UTC and (b) 12:00 UTC. SkewT-logp diagrams: the red bold line is temperature, the green line is the dew point and the orange bold line (above CLC) the wet saturated adiabat. Below LCL, we find the dry adiabat corresponding to the plotted temperature and dew point.

and the wind profiles over the sea close to Heraklion and Limnos do not show any significant differences in comparison with those at Naxos, so we can say that the structure of the PBL over the entire Aegean Sea during midday shows a shallow lowest mechanical turbulent layer and above it a temperature inversion up to about 1300 m witnessing the intense presence of the sea breeze. Even in big islands and mainland coasts, the wind coming from the sea affects significantly the PBL toward increasing its static stability (Helmis et al., 1995).

We have found so far that nowadays operational ECMWF IFS analyses realistically represent the initial structure of the PBL over the Aegean Sea, and the attempts are ceaseless by the stuff of physics section improving it (Sandu et al., 2020). Also, the well-known physical processes transferring scalar physical quantities inside the PBL contributing to the diurnal variation of the Etesian winds stressed once more. All these are in agreement, which verifies that when modifying the second running of the WRF model to completely stabilize the PBL the model did

not forecast the diurnal variation of the Etesian winds (Prezerakos et al., 2018).

3.2 A possible inertial oscillation in the Aegean Sea during summer and its contribution

The concept of the influence of nocturnal LLJ variability occurring just above the temperature inversion was introduced in international meteorological literature by Blackadar (1957). Thereafter, many researchers (cited in van de Wiel et al., 2010) have dealt with this physical phenomenon. The van de Wiel et al. (2010) study goes beyond Blackadar's aspects adding the notion that the ageostrophic wind vector rotates around the actual wind of its equilibrium state and because of the surface friction, the wind of the initial state reduces in an oscillation time-span. This oscillation can operate assuming that the diurnal cycle of the surface heating is strong, the PBL is barotropic and, of course, a physical system in motion being in an equilibrium will undergo an abrupt forcing.

In the Aegean Sea, in the case of Etesian winds type A, the nocturnal LLJ always exists, e.g., close to Naxos about 450 m height with 12 m s^{-1}. The 10 m wind force is 4 m s^{-1}. Over isles and sea, cooling from below occurs from sunset until sunrise and a nocturnal inversion forms with top just beneath the LLJ. The strong heating, of course exists in the isles in daytime, but as we have already mentioned in the previous subsection its influence is limited thanks to the air coming from the open sea, except for the large island and mainland south coasts. Over sea, the temperature diference increases thanks to warmer air and the cooling from bellow continuous resulting in the PBL structure depicted in Figure 3a. It is given that, although the weather is always fair, the rest of te conditions are not so favorable over Aegean as these at Cabauw for the IO to appear (van de Wiel et al., 2010). Firstly, there is no dramatically and abruptly change in the PBL stability and secondly the PBL is strongly baroclinic. Nevertheless, as there are many places in Greece where the radiation cycle is very intense and the complexity of the physical terrain upon the Aegean Sea is capable to produce easily a variety of gravity and inertial waves for playing the role of trigger effects, a more in-depth study of IO would prove very useful. It is now rather important to note that the present article does not aspire to improve the conceptual models of IO that have been proposed so far, but only to identify its possible contribution to the diurnal variation of the Etesian winds type A.

We mentioned above that when a type A Etesian wind occurs over the Aegean Sea, the geostrophic wind is almost constant mainly about the middle of its spell, being governed by the synoptic-scale pressure gradient, but the actual wind appears to be at surface subgeostrophic in night and supergeostrophic in day, whereas just above the mixing layer, the reverse. Consequently, for a better physical explanation of the phenomenon, our interest focuses on the diurnal variation of the geostrophic departure (ageostrophic wind). It is this part of the wind, which includes all the varying components of the atmospheric spectrum of motion being created by the pressure gradient belonging to smaller scales. For that reason, we use the complex number Z to denote the ageostrophic wind in the PBL, assuming of course, a barotropic state without the baroclinic local and regional thermal circulation. (Blackadar, 1957; Wiin-Nielsen, 1973).

With $Z=u'+iv'$ where $u'=u-u_g$ and $v'=v-v_g$ we get:

$$\frac{\partial Z}{\partial t} = \frac{\partial u'}{\partial t} + \mathrm{i}\frac{\partial v'}{\partial t} \tag{5}$$

Introducing in Eq. (4)

$$v_g = \frac{1}{f\rho}\frac{\partial p}{\partial x} \text{ and } u_g = -\frac{1}{f\rho}\frac{\partial p}{\partial y}$$

We get

$$\frac{\partial u}{\partial t} = fv - fv_g - \left[w\frac{\partial u}{\partial z} - \frac{1}{\rho}F_x\right],$$

$$\frac{\partial v}{\partial t} = -fu + fu_g - \left[w\frac{\partial v}{\partial z} - \frac{1}{\rho}F_y\right]$$

Therefore

$$\frac{\partial u'}{\partial t} = fv' - \left[w\frac{\partial u}{\partial z} - \frac{1}{\rho}F_x\right],$$

$$\frac{\partial v'}{\partial t} = -fu' - \left[w\frac{\partial v}{\partial z} - \frac{1}{\rho}F_y\right]$$

Then Eq. (5) becomes:

$$\frac{\partial Z}{\partial t} = \left[f v' - \left(w \frac{\partial u}{\partial z} - \frac{1}{\rho} F_x \right) \right] +$$

$$i \left[-f u' - \left(w \frac{\partial v}{\partial z} - \frac{1}{\rho} F_y \right) \right]$$

$$\frac{\partial Z}{\partial t} = f v' - i f u' - \left(w \frac{\partial u}{\partial z} - \frac{1}{\rho} F_x \right) +$$

$$i \left(w \frac{\partial v}{\partial z} - \frac{1}{\rho} F_y \right)$$

And setting

$$C = f \left[\left(w \frac{\partial u}{\partial z} - \frac{1}{\rho} F_x \right) + i \left(w \frac{\partial v}{\partial z} - \frac{1}{\rho} F_y \right) \right]$$

We get

$$\frac{\partial Z}{\partial t} = - i f \left(i v' + u' \right) - \frac{C}{f}$$

This means that:

$$\frac{\partial Z}{\partial t} = - i f Z - \frac{C}{f} \tag{6}$$

The solution of Eq. (6), as being a simple linear differential equation, is:

$$Z = C' e^{-ift} + \frac{iC}{f^2}$$

If $C' = Z_0$ is the ageostrophic wind at the initial time and C is the whole impact of the surface friction length and the vertically turbulence interchange of momentum, then the solution is:

$$Z = Z_0 e^{-ift} + \frac{iC}{f^2} \tag{7}$$

The solution given by Eq. (7) suggests that the vertical momentum transport affects strongly the wind inside a turbulent frictional layer. Neglecting this term, we get the solution

$$Z = Z_0 e^{-ift} \tag{8}$$

This solution is valid at the top of the temperature inversion. At this height, the flow is almost frictionless and horizontal, and the actual wind should show a local maximum at night, provided there is no loss of turbulent momentum downwards. Although it is not possible to verify this last aspect by observational data during the day for the baroclinic circulation (sea breeze), it cannot be eliminated physically since the weather is always fair. It is possible to do so during the night, given that the sea breeze has ceased and the land breeze is very weak, except for the big islands (e.g., Crete).

Thus, to plot the solution given by Eq. (8) we use the complex plane shown in Figure 4. The upper circle, with its center as the origin 0 of the coordinates,

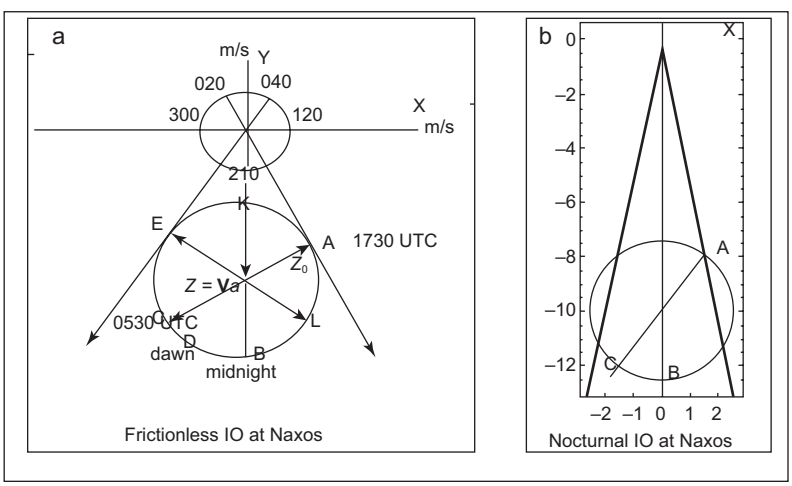

Fig. 4. (a) Complex plain showing the impact of a geostrophic wind on the actual type A Etesian winds at the top of the temperature inversion at Naxos. (b) Plotting of Eq. (8) solution with **V**g = 030º/12 m s^{-1} and initial actual wind $\mathbf{V}_0$ = 020º/8 m s^{-1}.

is the well-known one presenting the directions of the winds in degrees. In addition, we treat the winds in the northern sector as being negative and those in the southern sector as positive. Following the findings of the present study, we identify the amplitude of the wind waving direction between 040º and 020º. Also, the wind similar to a low-level jet seen in Figure 4 is located at 750 m height, where the top of the temperature inversion is. At this height an almost frictionless drag layer exists with subgeostrophic winds during the day. However, winds are supergeostrophic during the night, since the turbulence drag ceases and the wind accelerates after sunset, reaching a balanced state later. The lower circle is tangent to an angle of 20 degrees, which is just the mentioned amplitude. This circle's radius is the absolute value of Z circulating along the periphery of this circle in a clockwise direction with a period of a half pendulum day being $T = 2\pi/f$ (AMS, 2018).

Here Z_0 is the value of Z at $t = 0$. The period T of the oscillation being the half of a pendulum day is 20 sidereal hours, since the pendulum day at the vicinity of Naxos at latitude 37.1º is 40 sidereal hours. We can say that Z pointing at A on the complex plain seen in Figure 4 determines the actual wind at the initial time. Vector Z, moving clockwise, makes a complete circle in 20 sidereal hours. This means that five sidereal hours are equivalent to six conventional hours. When Z targets point B, the actual wind adopts its maximum force and then reduces gradually. When it targets point K the actual wind adopts its minimum force, but never reaches it since the oscillation after dawn stops functioning. To correspond exact time to the points A, B, C, D and E of Figure 4 we have first to determine the UTC time at A ($t = 0$), which is the sunset time 17:30 UTC. At C after 10 sidereal hours the time is 17:30 + 12 = 05:30 UTC of the next day. EL is perpendicular to OE, thus at L is 20:33 UTC and at B is 00:10 UTC. At D, the time is 03:30 UTC, which is about the time of sunrise and the turbulent drag starts reappearing. At E, the time is 06:50 and at K is 12:10 UTC. The inertial oscillation is working during a part of its period, namely from sunset (17:30 UTC) to sunrise (03:30 UTC).

The situation at Naxos is similar to that for nearly all meteorological stations on the Aegean Sea with, of course, a few differences corresponding to their locations, which determine the direction and intensity of the sea breeze circulation and its diurnal variation. The plot of Eq. (8) solution is exactly the same with Blackadar (1957), yet the numerical example shown in Figure 4b uses $Vg = 030º/12$ m s^{-1} and actual wind of 020º/8 m s^{-1} at 17:30 UTC). In this numerical example the amplitude of Z has been calculated by cosine low and for that reason the sides of angle a cross the radius Z circle. The angles corresponding to Limnos and Iraklion are much greater than those shown in Figure 4, meaning that with same geostrophic wind force the ageostrophic wind at these two locations is much greater than the one at Naxos.

In order to plot the Eq. (7) solution, we follow van de Wiel et al. (2010), who studied the nocturnal inertia oscillation considering the friction, but constant in nighttime. This assumes an equilibrium state between pressure gradient, Coriolis force and all kinds of frictional forcing at a time during the night, around which the initial wind vector executes a clockwise circular motion. Because of the continuous alteration of possible damping and external forcing, this state is almost impossible to be determined or does not exist; thus, they adopted equilibrium states resorting to Ekman's spiral equations and the center of mass indicated by observations. Furthermore, knowing all the physical processes and also their interactions and variations, they mentioned most of them and they also cited the research papers dealing with these matters. After these remarks they used the well-known relation to transform Eq. (8) solution:

$$cosn\theta + isinn\theta = (cos\theta + isin\theta)^n = e^{in\theta}$$

Then we have:

$$u - u_{eq} = \left(v_0 - v_{eq}\right)\sin(ft) + (u_0 - u_{eq})\cos(ft)$$

$$\left(v - v_{eq}\right) = \left(v_0 - v_{eq}\right)\cos(ft) - (u_0 - u_{eq})\sin(ft) \qquad (9)$$

where u_0, u_{eq}, v_0 v_{eq} are the initial and equilibrium values, been determined in association with the frictional effects (diffusion in the PBL) as mentioned just above. The difference between the initial and equilibrium states of wind values is the ageostrophic wind small in magnitude considered constant during the night, but its clockwise revolution about the equilibrium state makes the actual wind to reduce.

Another restriction we have to consider is that the direction of Etesian winds at the surface (10 m height) appears to wave between 340º and 20º, at least close to Naxos. In addition, the equilibrium occurs at night after the initial time being at 17:30 UTC. The vector **OA** (Fig. 5a) denotes the wind at sunset (17:30 UTC). the author's estimation, based on the available data but also on his synoptic experience, is that after this time the downward transport of momentum gradually decreases the wind force due to surface friction and after a while (19:30 UTC) adopts its equilibrium **OK** value, denoted by point B. Then we get the amplitude of ageostrophic wind **KA**. This ageostrophic wind rotates around K from point A (sunset) until point S (sunrise about 03:30 UTC). The period of inertial oscillation is 20 sidereal hours but after about 6.6 sidereal hours it stops. Figure 5b depicts the plot of Eq. (9) solution setting $\mathbf{V}_0 = 330º/16\ ms^{-1}$ and $\mathbf{V}_{eq} = 360º/8\ m\ s^{-1}$. The points of the curve are the ends and point O, origin of coordinates, the beginning of the actual wins vectors. This example verifies completely the analysis of Figure 5a.

The theoretical process followed to reach Figures 4 and 5 and the fact that in the Aegean Sea, except for the rather sudden total stabilization of the internal boundary layer in the evening, many other trigger effects can disturb the balance of the airflow anytime, providing the possibilities of an inertial oscillation to start. However, the direction of Etesian winds shows, as we have already mentioned above, very limited variation, which is the main characteristic of the inertial oscillation. The last effect makes us to point out that for synopticians the inertial oscillation over the Aegean Sea would not keep great interest.

3.3 Local and regional secondary baroclinic circulation and its contribution

During the day, inside the entrainment zone just above the mixing length, an LLJ is set. The position of the jet is lifted in comparison with the nocturnal one, but weaker according to inertial oscillation is much stronger than the nocturnal one, as well. This fact, to author's opinion, witnesses the presence of the local and regional sea breeze circulation.

In order, the main characteristics of the land-sea breeze to be found out many studies have been carried out. Many scientists have worked theoretically and observationally at various positions in Greece and mainly in Attica, the major region, where Athens belongs to (Zambakas, 1973; Prezerakos, 1986; Helmis et al., 1987; Steyn and Kallos, 1992; Varvayianni et al., 1993a, b; Melas et al., 1998a, b). The last two should be considered as particular valuable for being coupled by experimental observations having been archived and thus the studies can be repeated nowadays utilize the latest version of WRF model to result in more realistic findings at many places (grid points). The sea breeze in Thessaloniki was studied by Sahsamanoglou (1976) and also, two rather recent investigations (Papanastasiou and Melas, 2009;

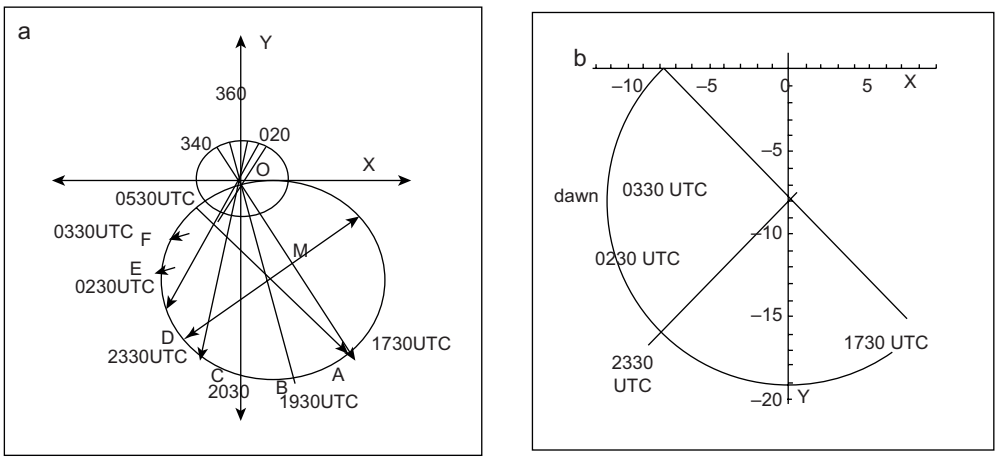

Fig. 5. (a) Plot of Eq. (9) for Naxos 10-m wind. OK is the equilibrium wind state at 19:30 UTC and OA the initial state at 17:30 UTC, while KA is the ageostrophic wind rotating around K. (b) Numerical example of Figure 5a plot setting $\mathbf{V}_0 = 330º/16\ m\ s^{-1}$ and $\mathbf{V}_{eq} = 360º/8m\ s^{-1}$.

Papanastasiou et al., 2010) having used the WRF model studied in detail the sea breeze over the complex terrain in the Volos region (Fig. 1) with significant findings. The study, which focuses on sea breeze over the Aegean Sea is the only one by Repapis and Mantis (1980) investigating first of all the coexistence of sea breeze and Etesian winds based on the harmonic resolution of the pressure diurnal variability.

In the just above-mentioned studies, the bulk work of Costas Pikros must be included (Pikros, 1976; Prezerakos and Pikros, 1989; Pikros and Prezerakos, 2006). Pikros (2000) whole work, mostly not published, is recorded in his website where valuable information about sea and mountain breezes for almost all Greece can be found.

We have already mentioned in the introduction the difficulty appears the spectrum of the atmospheric motion scales be resolved by dynamical and parametrized physical processes for each scale being studied separately. However, this is possible in few cases. The most known is when synoptic-scale gradient wind is an offshores one as it happens in many positions in Greece. Therefore, detailed studies of the pure sea breeze at most of these positions have managed selecting days with a very smooth barometric field (Prezerakos, 1986; Melas et al., 1998a). This difficulty remains over the central, eastern Aegean Sea and north Crete, where mostly the directions of sea breeze and Etesian winds coincide. Over these areas, the only physical phenomenon capable to cease the function of radiation cycle and as a consequence the sea breeze, is an overcast ceiling, which rarely happens. Also, over the southeastern part of Aegean Sea, which is steadily under the influence of Cyprus low a significant pressure gradient always exists resulting in ceaseless Etesian winds.

The operational meso-scale models are capable to predict satisfactorily the local and regional thermal air circulation and its diurnal variation (Helmis et al., 1987; Kambezidis et al., 1998; Melas et al., 1995, 1998a, b; Papanastasiou and Melas, 2009; Papanastasiou et al., 2010; Varvayianni et al., 1993a, b). Of course, it is a little bit difficult to discriminate it from the background pressure gradient one, mainly when they get the same direction.

There are many cases that the synoptic scale MSLP field is uniform over Aegean Sea and the day time synoptic observations show clearly this thermal baroclinic circulation except for the eastern Aegean Sea south of Limnos where Etesian and regional circulation get the same direction. Figure 6 illustrates such a case and in the same time it appears to be compatible with Figure 1, where the big arrows denote the regional thermal gradient, whereas the small arrows the local ones. One of the major reasons that the diurnal variation of sea breeze hodograph shows an anticlockwise (backing) rotation, in many seaside places, contrary to Coriolis force (Zambakas, 1973; Prezerakos, 1986; Steyn and Kallos, 1992) is that in the course of the day the regional thermal circulation prevails usually the local one.

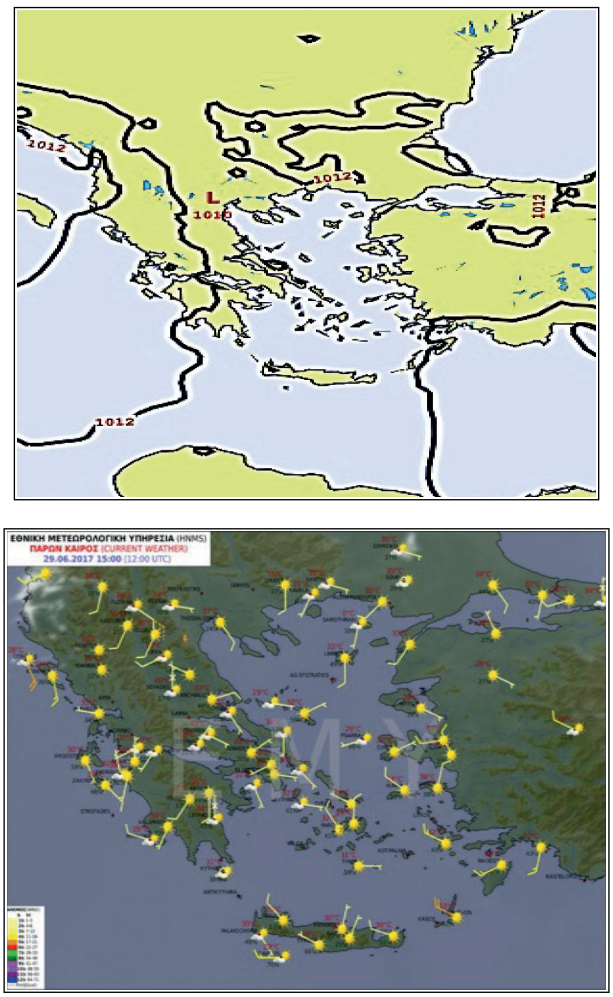

Fig. 6. Top: MSLP field, isobars per 4 hPa. Bottom: wind, temperature and cloudiness, on June 29, 2017 at 12:00 UTC. Wind velocity is plotted by WMO conventional way, one barb = 5 m s^{-1}.

Applying the Bjerkness' circulation theorem (Holton and Hakim, 2013; Wiin Nielsen, 1973) and utilizing the simplified result we find

$$DV/Dt = [R \ln (p_0/p_1)/ 2(h + L)] (T_2 - T_1) \quad (10)$$

We put into Eq. (10) the air temperature difference between over cold sea just south of Limnos (25º E, 39º N) and the southwest of Asia Minor (29º E, 37º N), $T_2 - T_1$=15 ºC (mean from surface up to 900 hPa), p_0 = 1004 hPa, p_1 = 900 hPa, h = 1000 m. $L = 484 \times 10^3$ m (L is the distance between the points (25º E, 39º N) and (29º E, 37º N) calculated by the equation of spherical trigonometry:

$$\cos L = \sin\varphi_1 \sin\varphi_2 + \cos\varphi_1 \cos\varphi_2 \cos (\lambda_1 - \lambda_2) \quad (11)$$

where (λ_1, φ_1), (λ_2, φ_2) are the geographical coordinates respectively of the points under consideration and L the arc length of a great circle of the Earth passing through these two places. Thereafter, we find DV/Dt = 0.0004812 m s^{-2}, where V is the amplitude of the mean tangential velocity along the circuit of the sea breeze. This acceleration produces V = 10.4 m s^{-1} in 6 h. This wind force is frictionless, but in reality, as the wind speed increases with time, the frictional force reduces the acceleration rate, and temperature advection reduces the land-sea temperature contrast so that a balance is obtained between the generation of kinetic energy by the pressure density solenoids and frictional dissipation. This balance keeps almost steady until the sunset. This sort of baroclinic circulation appears frequently thanks to the development of distinctive intra-urban surface thermal patterns reported by Agathangelidis et al., (2020) in 25 European cities with Athens included, aggregating their findings to similar ones of so many Greek, and not only scientists mentioned broadly above. Similar circulation should be tested over the open sea when a distinct gradient appears in SST, as this between North Aegean and Karpathion Seas or Antalya's gulf and Middle East coastal waters. The impact of these sub-synoptic SST gradients on the synoptic scale atmospheric circulation is waiting to be studied separately. All this scientific information set here about sub-synoptic scale baroclinic circulation occurring over the Aegean Sea is intended to reveal its close correlation with the diurnal variation of the Etesian winds type A.

3.4 Numerical experiment. Initial values: NCEP-GFS on July 24, 2020 at 00:00 UTC.

Although the contribution of the local and regional sea breeze to the diurnal variation of the Etesian wind type A has become, so far, more than clear, a numerical experiment is necessary to test this aspect. The original motivating thought was "what should happen if we manage to eliminate the physical mechanism, which is responsible for the genesis of the secondary 2-m temperature gradient during the day?" We executed a numerical experiment utilizing once more the WRF-ARW v. 4.0. We selected two domains, one covering most of Europe, North Africa, Asia Minor and most parts of Middle East with a 9-km horizontal grid increment and an inner domain covering Greece and Asia Minor with a horizontal resolution of 1.8 km (Fig. 7). We disseminated vertically 51 unevenly sigma levels with the top level at 5 hPa and 18 levels up to 2000 m. The parameterizations used for this experiment are the same than those having outputs in Figure 3a, b. This time, the necessary initial analysis was forced to the model at 00:00 UTC on July 24, 2020 and the initial and lateral boundary values were provided every 6 h by the NCEP-GFS in a horizontal resolution of 27 km. The integration time step of the running model is 10 min and the outputs are saved every 1 h. The simulation lasted for 48 h until 00:00 UTC on July 26, 2020 and two simulations were performed full physics (full) and no full physics (nofflx). The

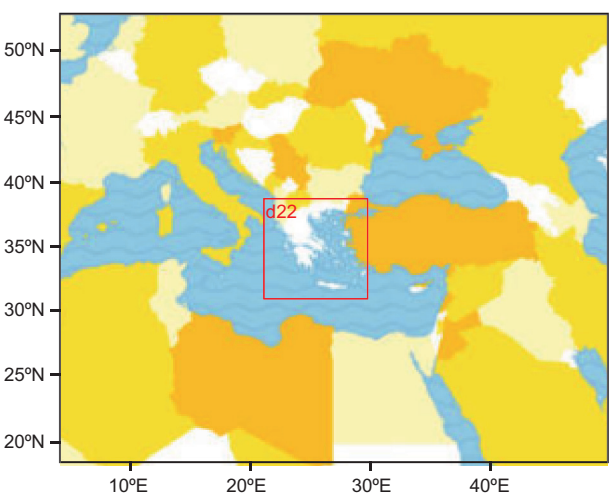

Fig. 7. Domains used for running the WRF-ARW v4.0 for the numerical experiment.

results coming from this numerical experiment are impressively interesting.

We start our analysis with the synoptic conditions during the two-day period of the experiment as derived from surface observations and the model outputs from the first numerical simulation using full physics. These two days (24 and 25 July 2020) belong to the Etesian winds type A group, since moderate to strong Etesians blow over the Aegean Sea and no sea breeze appeared at Hellinikon and National Observatory of Athens (NOA) meteorological stations. Moreover, an inspection of European surface synoptic analyses available at the German National Meteorological Service (Deutscher Wetterdienst, 2020) website, certified that in the time period from 20 to 31 July, 2020 no Etesian winds outbursts occurred. In other words, the high-pressure field over the Balkans was remaining smoothly steady during this time with the exception of the light fall of synoptic scale pressure due to the passage of a 500 hPa trough at about 00:00 UTC on July 25 and one ridge about July 28. The light pressure fall was added to this due to ground radiation resulting in weakening of the Etesian winds and intensifying of the sea breeze at 12:00 UTC. In addition, local sea breeze occurred in the South Peloponnese, in the north coasts of Greece and at the west coasts of Asia Minor. At 12:00 UTC on July 25, a narrow lane with 8 hPa value and no gradient characterized the MSLP field distinctly. This lane divides the Aegean Sea into two parts, the west part influenced by the Greece mainland and the east one influenced by Western Asia Minor. The MSLP value is decreasing about 12 to 10 hPa from north to south over the mainland of Greece, while over Asia Minor west of 29º E the MSLP ranges between 1010 and 1004 hPa, decreasing southwards with the lowest values east of Rhodes Island. This means, in turn, that Greece is under the influence of the Balkan anticyclone and Asia Minor of the Persian trough (Prezerakos, 2022). The difference between night and day, that is 00:00 and 12:00 UTC makes sense not only above land, where the pressure decreases as expected at 12:00 UTC, showing its strong dependence of the underlying terrain temperature change, but even an equivalent rising over sea. This is shown clearly by Figure 8a, where daytime minus nighttime pressure is positive evenly distributed over sea and negative oddly distributed over land. The main inference arising here is that the MSLP alters simultaneously and reversely at the edges (over sea-over land) of the closed panel of sea breeze circulation. Figure 8b shows the same difference in nofflx simulation. The difference values are almost the same over open sea, but of opposite sign over land and waters close to land, more than 2 degrees lower, only when the offshores direction is toward south. Over main lands

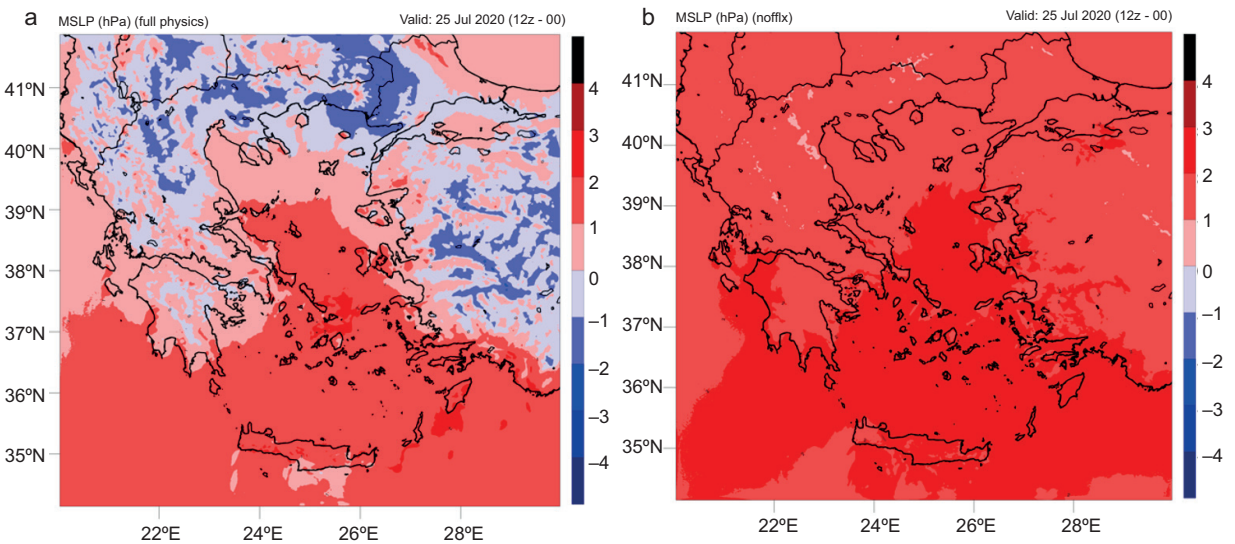

Fig. 8. (a) ARF model (full), (b) nofflx simulation MSLP difference forecasts at 12:00-00:00 UTC/ July 25, 2020.

and large islands, during the night, the temperature at 2 m is about 22 ºC, a little bit colder than the coasts. Thereafter, the land breeze is light, and the katabatic winds are stronger due to much lower temperatures over the mountains and ground sharp inclination, without extension to the open sea, but affecting the coastal meteorological stations (Helmis et al., 2002). At midday, the 2-m temperature increases from 22 to more than 36 ºC resulting in a settlement of the temperature gradients inside the PBL with the simultaneous accumulation of eddy potential energy. The author has expressed, many times, the aspect that the trigger effect for starting the conversion of eddy potential energy to kinetic seems to be a critical mean value in the space box of the expected circulation. This conceptual aspect has waited for a long time for a prompt scientist to study it fully and in depth even for all scales of atmospheric circulation.

The distribution of the 2-m air temperature over the sea remains the same during the day and night in agreement with the SST analysis. The colder sea area with values ranging from 20 to 24 ºC spreads from the northeastern coasts of Greece to south of Naxos, as the SST of July 25, 2020 shows (Fig. 9a). This low SST is due to the cool water from the Black Sea and coastal upwelling driven by the strong northeasterly Etesian (Mavropoulou et al., 2016). The distribution of SST over all of the Greek waters is depicted in

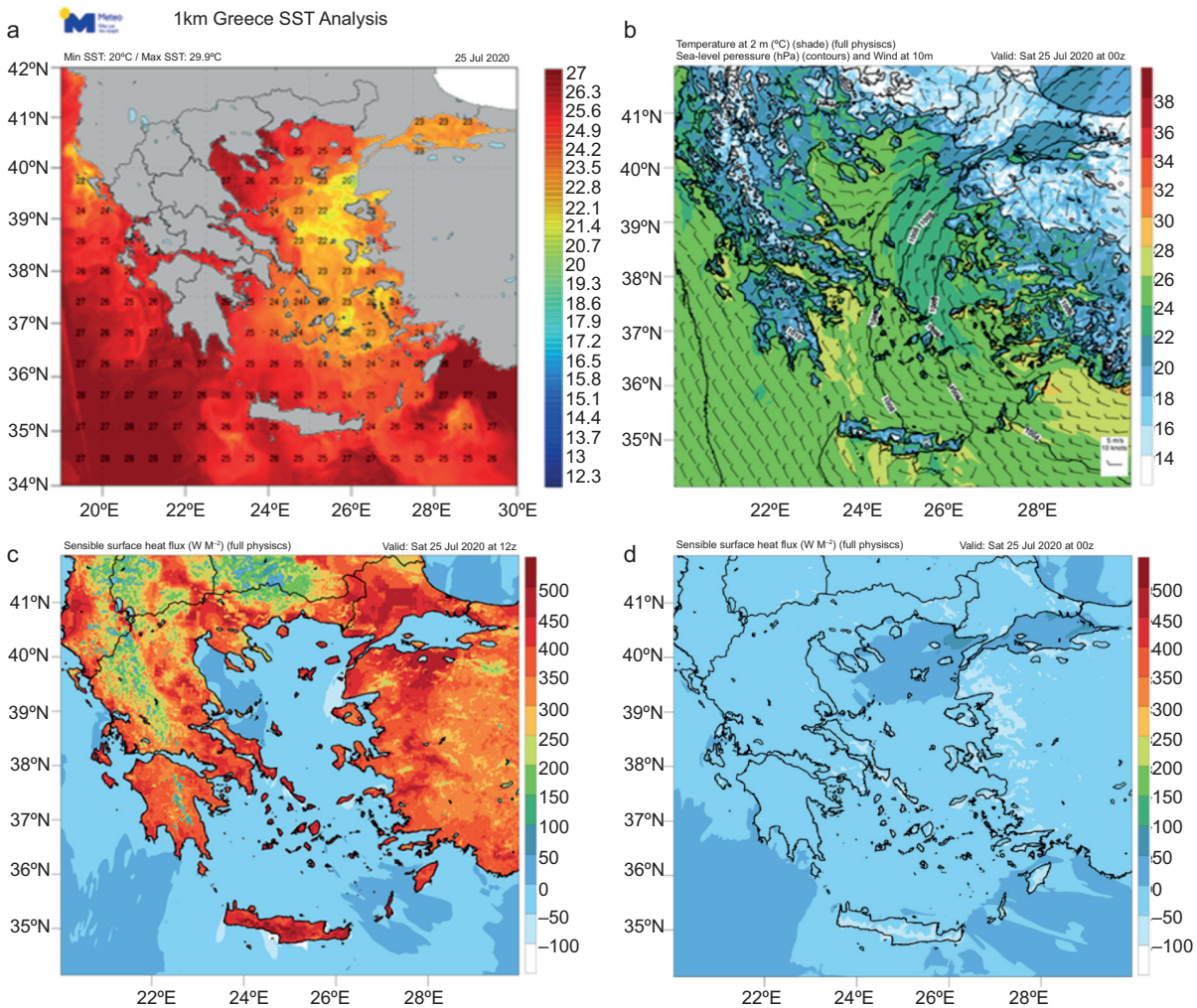

Fig. 9. (a) Sea surface temperature, (b) MSLP wind and 2-m air temperature at 00:00 UTC, (c) at 12:00 and (d) sensible surface heat flux at 00:00 UTC on July 25, 2020.

Figure 9a ranging from 20 to 29 ºC. The highest SST value appears over the southeastern Aegean Sea close to the Turkey coast. The 2-m temperature over the open sea ranges between 22 and 26 ºC in night. The 2-m temperature close to the coastal waters is 1 to 2 ºC lower (Fig. 9b). A comparison between Figure 9a, b justifies what has already been mentioned in section 3.2 about the slightly positive sensible heat flux in a few areas of the Greek waters even at night (Fig.9c, b).

Thus, during the night over the northeastern part of the Aegean Sea the air is coming from the Sea of Marmara as a northeasterly wind, which splits at 39.5º N into two parts. The eastern part follows a cyclonic circulation around Asia Minor, while the western part an anticyclonic path around North Greece. This circulation alters to NNE, just south of Sporades, passing over Euboea and Attica, becomes NW keeping this direction as far south as in Crete. The comparison between the midnight and midday wind fields reveals the contribution of sea breeze to the diurnal variation of the Etesian winds type A. Since we will study this contribution in details later, here we can only say that the model findings, so far, verify the inferences appearing in subsection 3.3.

The most effective tool in the author's opinion, which is capable to show clearly the impact of sea breeze circulation, is the difference in the 10-m wind fields at 12:00 UTC coming from the full-physics simulation minus the idealized simulation (nofflx). In this formula "full" denotes a product of the model running regularly and "nofflx" a product of the same model running without the simulation of the physical mechanism, which produces the land-sea baroclinic circulation.

Figure 10 shows effectively this difference. Colored calibration refers to the wind force difference only and the arrows denote the vector difference of the wind. We can estimate accurately the amplitude of the vectors considering the 5 m s^{-1} =10 kn sample depicted at the bottom right corner of Figure 10. With a simple simultaneous glance at the color hints and the white vectors, we can realize where the sea breeze occurs and how much it affects the synoptic scale wind. The vectors directed from south onshore in red color hint means that this vector is the sea breeze, much greater than the contrary Etesian wind. The similar vectors in blue hints are sea breeze weaker than the

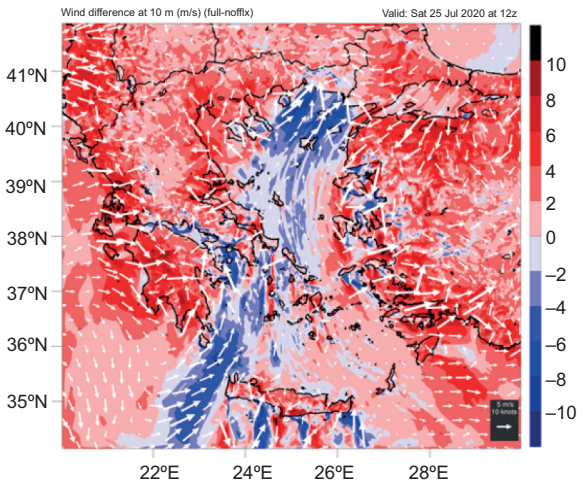

Fig. 10. Color contours: wind force scalar difference (full-nofflx) per 2 m s^{-1}. White vectors: wind velocity vector difference (full-nofflx) according to the sample measure displayed at the bottom right corner (5 m s^{-1} =10 kn) on July 25, 2020 at 12:00 UTC.

contrary Etesian as well. Such an area with thermal air circulation coming from south covers all the north Aegean Sea and the west part of the rest, even Saronic Gulf, details that we can easily get from Figure 10 following the just above-mentioned rule. Thus, over the eastern part of the Aegean Sea south of 39º N, the sea breeze enforces the Etesian winds, but the complexity of surface terrain affects it significantly in many ways. So, reaching Asia Minor and particularly these parts with the highest 2-m temperature the sea breeze gets its intensity maxima, e.g., at just NE of Rhodes island. In central Aegean open sea, the influence of the breeze seems to be trivial; however, close to the large islands the appearance of the local sea breeze makes sense, where at the north coast it enhances (red) Etesian and at south ones enfeebles it (blue). Great concern presents the case of big island Crete. At its north coasts the sea breeze blows from north enforcing Etesian, so in Figure 10 these coasts appear to be red. At south coasts sea breeze is coming from south contracting Etesian. The Etesian winds flow is disturbed significantly by Crete (Kotroni et al., 2001), resulting in a waving of Etesian force per lane shape areas. Over blue lane areas sea breeze is stronger than Etesian witnessing that these areas are south of high mountains. Over red ones Etesian is stronger than sea breeze witnessing that Etesian

comes here passing through low-level ground being between mountains. Similar picture displays at all the large islands. The last region deserving mention is the southwest part of Greece. Just east of Crete, in open sea, a blue lane denotes that the 12:00 UTC full Etesian is much weaker than the nofflx Etesian. The study of the two wind fields separately verifies this aspect. Firstly, we examine the full wind field. This blue relatively cold sea surface region is a wind convergence, where the northwest flow coming from Ionian meets the Etesian northeasterly. Simultaneously, this region is the starting place of two sea breezes one northward to Peloponnesus and the other southward to Crete resulting in an almost calm wind field. In the other hand over the same region, the nofflx wind field is undisturbed with northeasterly flow.

Figure 10 provides numerous inferences to prove the contribution of sea breeze to the diurnal variation of Etesian winds type A. However, although the main goal of this paper seems to be succeeded, some more demonstration is necessary to advocate it. Although Figures 10 and 11 would be expected similar to each other, they display some variations. Before we attempt to elucidate them, we have to interpret the sort of atmospheric circulations that the Figures display. The nofflx meteorological fields during the whole simulation time are almost unchanged following the initial values influenced slightly by the lateral boundary values. We can say that the nofflx wind field is the sum of the Etesian wind and the 00:00 UTC on July's 24, 2020 land breeze. Therefore, its time small variations seen in a variety of places (Fig. 12) are Etesian winds variations or IO and mechanical turbulence. The author's aspect is that WRF-ARW is very sensitive to the transformation of the flow from balance to unbalance responding to an IO starting. Really, Figure 12 shows almost zero to slight differences, which could be attributed to mechanical turbulence and/or nocturnal IO except for the southwest part of Greece. As we have already justified the existence of the blue lane field in Figure 10, we are able to explain the red color of almost the same region. As both wind fields are nofflx, the red color means that the nighttime northerly is stronger than the previous daytime one. The resulting difference is due to synoptic scale pressure gradient or to nocturnal IO, since the land breeze difference is zero. Looking at both fields separately we realize that the winds at 12:00 UTC have changed mostly to south-southwest. This usually occurs when a subtropical anticyclone extends from south toward Greece. It is now time to address the differences between Figures 10 and 11. Figure 11 depicts a wind difference field, which can be adopted easily by two initial analyses or reanalyses with better results than these of the forecast fields in Figure 11. In both figures the wind differences shown correspond to sea breeze, except for the southwest part for the above-mentioned reasons.

Finally, the WRF provides us the facility to investigate the state of the PBL and its evolution over the Aegean Sea during the simulation time. The detailed

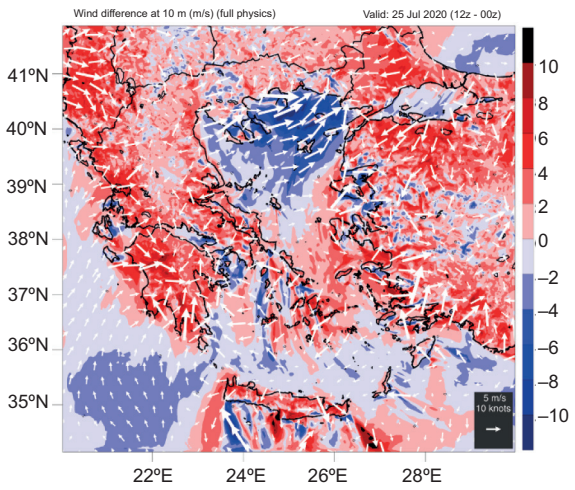

Fig. 11. As Figure 10, but for the difference (12:00-00:00 UTC) of full physics simulation.

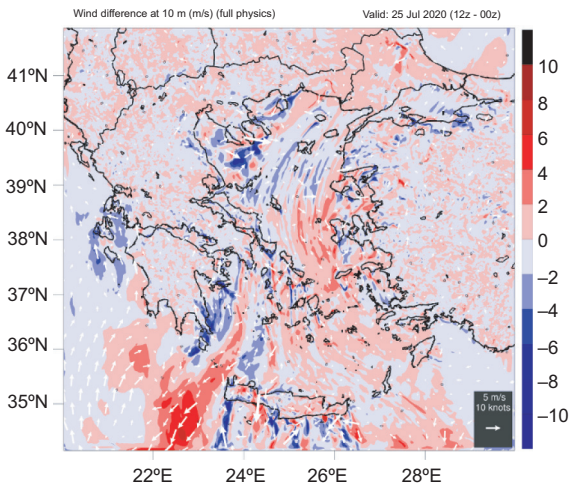

Fig. 12. As Figure 11, but for the nofflx simulation.

study of Figures 13 and 14 reveals the variation of the wind inside the PBL and its entrainment up to 650 hPa. Speaking generally, we can remark that during all of the time of both simulations, at the central Aegean Sea the entrainment is characterized by strong synoptic scale subsistence with maximum values about 0.2 m s^{-1} appearing at about 750-hPa. Beneath the mesoscale 850-hPa, ascending occurs, increasing gradually and reaching its maximum at about 500 m lifting at midday at about 750 m. The low-level jet appears to be just below the ascending maxima witnessing clearly the presence of sea breeze in daytime and the mechanical turbulence all time. Figures 13 and 14 verify with certainty what was exposed in subsection 3.1 about the PBL over the Aegean Sea.

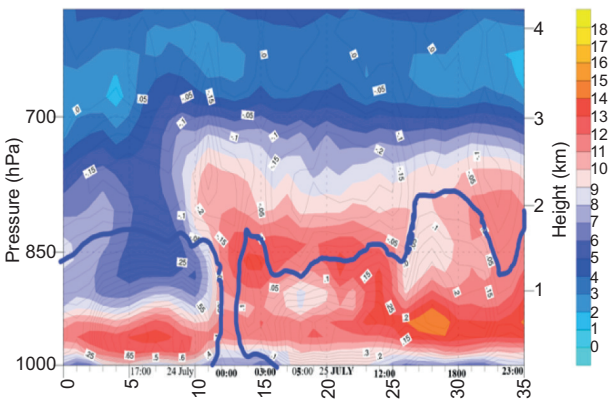

Fig. 13. Time-height cross-section of horizontal wind force V and the synoptic scale vertical motion w at Naxos. V color contours per 1 m s^{-1}, w black thin contours per 0.05 m s^{-1}. The thick blue line is the 0.0 m s^{-1} w contour. The horizontal coordinate axis denotes the 36 h of full physics simulation from July 24, 2020 at 12:00 UTC to July 25, 2020 at 24:00 UTC.

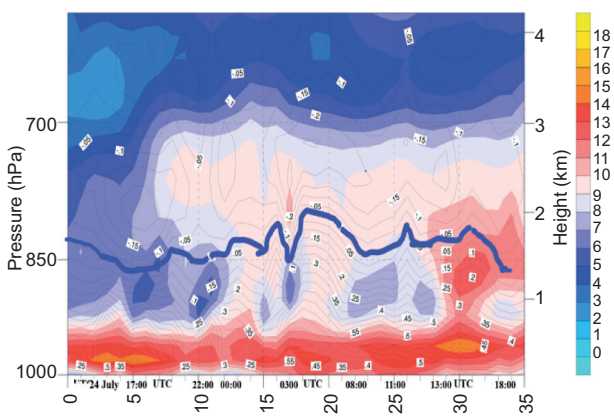

Fig. 14. As Figure 13, but for the nofflx simulation.

The theoretical approach, the adequate use and study of real time data and the numerical experiment revealed the way and extension in which the PBL, the nocturnal IO and the secondary thermal baroclinic circulation contribute to the diurnal variation of the Etesian winds type A.

4. Conclusions and suggestions for future research

After introducing the concepts of the three types of Etesian winds (A, B, and C) blowing over the Greek seas during summer, we present a few simple statistical elements of types A and C. Then, a theoretical investigation was made for finding out the atmospheric physical processes, which are responsible for the diurnal variation of Etesian winds type A. Eq. (7) revealed that the physical factors which contribute to the observed wind variability are included in the so-called ageostrophic wind. It is this part of the wind, which includes all the varying components of the atmospheric spectrum of motion being created by processes belonging to smaller scales, namely orography, distribution of sea-land, PBL state including sub grid mountain drag, vertical exchange of momentum and heat by mechanical and thermal turbulence. The abrupt change of the PBL flow from balanced to unbalanced forces the initiation of the nocturnal IO, while the solar-earth surface radiation cycle creates the necessary temperature gradient for the local and regional secondary PBL baroclinic circulation.

The research in order to identify the structural characteristics of the PBL over the Aegean Sea used the ECMWF IFS HERL analyses transferred to the WRF-ARF model for executing the numerical diagnosis, which revealed the maritime mostly stable, but turbulent nature of the PBL. The quantitative study of the PBL identified a nocturnal low-level jet at the layer between 400 and 600 m. In daytime, this wind force maximum lifts at about 750 m height interacting with sea breeze. The location of this low-level jet is just above the top of a temperature inversion existing usually in a maritime summer PBL.

The theoretical approach revealed that the solution of Eq. (7) simulates the atmospheric motion

inside the PBL during an ordinary day of Etesian winds type A. The complex unknown variable Z denotes the ageostrophic wind and $Z = u' + iv'$, where $u' = u - u_g$ and $v' = v - v_g$. This solution function by the term iC/f^2 denotes all the physical processes appearing in the PBL. The plot of this function is illustrated by Figure 5 and the function, which simulates the IO at the top of temperature inversion, where the low-level jet exists and no friction drag appears, is illustrated by Figure 4. Although the theoretical approach together with the study of real data and reanalyses provide many evidences for the function of the nocturnal IO over the Aegean Sea, one specific observational campaign is necessary to give the final certification.

Since the theoretical and observational study of the secondary thermal baroclinic circulation is almost satiated, even in Greece, we have devoted a significant part of this research to select all scientific information existed, so far, about local and regional land-sea breeze over the Aegean Sea. In addition, the author's synoptic experience together with the execution of numerical experiments via WRF-ARF contributed to the attempt, the close correlation of this sub synoptic circulation with the diurnal variation of the Etesian winds type A to be revealed and to be studied.

Given that the vertical exchange of the scalar quantities inside the PBL participates in the configuration of the wind profiles, we referred to a numerical experiment executed by Prezerakos et al. (2018) to verify these aspects. This experiment using the WRF-ARF and running it from 00:00 UTC on July 26, 2016 to 03:00 UTC on July 29, 2016 and modifying the second running of the model stabilizing the PBL completely, the model did not forecast the diurnal variation of the Etesian winds.

Finally, the execution of the numerical experiment using the WRF-ARF v. 4.0, which fed with GFS data, running it from 00:00 UTC on July 24, 2020 to 24:00 UTC on July 25, 2020 proved very effective. In this experiment, we modified the model's simulation for the second running, succeeding to turn off both the sensible and latent heat fluxes from the surface, stopping the function of the diurnal radiation cycle. As expected, the creation of the temperature gradient in the PBL ceased, hence the secondary baroclinic circulation. This WRF model's modification to the author's best knowledge was done for first time, at least in Greece, and the quantitative comparison of the two runs outputs proved manifestly that the local and regional thermal baroclinic circulation is the main physical contributor to the diurnal variation of Etesian winds type A. The second one is the structure and the subgrid scale processes of the PBL and the last one is the nocturnal IO, which needs more observational research to be certified completely. The WRF-ARF v. 4.0 48 h running provided us the chance to study the state and evolution of the PBL over the central Aegean Sea during two whole days. The inferences derived from Figures 13 and 14 depicting the relevant running outputs verify with certainty what we exposed in subsection 3.1 about the PBL over the Aegean Sea.

During this investigation we discovered unexpectedly that in rare cases the SST in very few areas of the Aegean Sea is slightly greater than the 2-m air temperature. This difference results in a sensible heat flux not more than 50 W m^{-2} during the day and night. Thereafter we have to suggest a separate study dealing exclusively with this matter. Moreover, we feel the need to propose that the subject of this research needs more in-depth study, utilizing real time data available by observations, at least up to 2 km, made by the adequate very sensitive instruments (Stull, 1988), set on drones. This kind of observational data are necessary not only to verify the findings presented in this article, but also for improving the PBL parametrization schemes over the Aegean Sea.

Acknowledgments

This research has not received any specific grant from funding agencies in the public, commercial, or not-profit sectors. The author would like to thank Dr. Stavros Dafis for his valuable contribution to this research. He executed the 2020 numerical experiment via the WRF-ARF model and revised the manuscripts. Also, the author would like to express his gratitude and deep appreciation to Dr. Michail Diamantakis for another revision of this paper. Additionally, ECMWF, NCAR and HNMS deserve acknowledgemnet for the provision of data, as well as the anonymous reviewers for their constructive comments, and Drs. Vassiliki Kotroni and Kostas

Lagouvardos, research directors at the National Observatory of Athens, for introducing Dr. Dafnis and steadily supporting this research.

References

Agathangelidis I, Cartalis C, Santamouris M. 2020. Urban morphological controls on surface thermal dynamics: A comparative assessment of major European cities with a focus on Athens, Greece. Climate 8: 131. https://doi.org/10.3390/cli8110131

AMS. 2018. Inertial flow. In: AMS glossary. Available at: http://glossary.ametsoc.org/w/index.php?title=Inertial_flow&oldid=16862

Andreakos K, Prezerakos NG, Xirakis P. 1984. Analysis of the airfield in Athens. Final report of B6612/9 contract number project prepared for the Hellenic Ministry of Physical Planning, Housing and the Environment, Athens.

Arrillaga JA. 2020. Thermally-driven mesoscale flows and their interaction with atmospheric boundary layer turbulence. Ph.D. thesis. Universidad Complutense de Madrid, Departamento de Física de la Tierra y Astrofísica, Madrid, Spain pp 165.

Arya SPS. 1985. The schematics of balance of forces in the planetary boundary layer. Journal of Applied Meteorology and Climatology 24: 1001-1002. https://doi.org/10.1175/1520-0450(1985)024<1001:TSOBOF>2.0.CO;2

Asimakopoulos DN, Helmis CG, Petrakis M, Tombrou M. 1993. Atmospheric boundary layer field measurements over coastal areas. Environmental Software 8: 9-18. https://doi.org/10.1016/0266-9838(93)90004-2

Asimakopoulos DN, Helmis CG. 1994. Recent advances on atmospheric acoustic sounding. International Journal of Remote Sensing 15: 223-233. https://doi.org/10.1080/01431169408954066

Blackadar KA. 1957. Boundary layer wind maxima and their significance for the growth of the nocturnal inversion. Bulletin of the American Meteorological Society 38: 283-290. https://doi.org/10.1175/1520-0477-38.5.283

Cahuich-López MA, Mariño-Tapia I, Souza AJ, Gold-Bouchot G, Cohen M, Valdés Lozano D. 2020. Spatial and temporal variability of sea breezes and synoptic influences over the surface wind field of the Yucatán Peninsula. Atmósfera 33: 123-142. https://doi.org/10.20937/ATM.52713

Carapiperis LN. 1955. On the frequency of the consecutive days with etesian wind. Proceedings of the Academy of Athens 30 (in Greek).

Carapiperis LN. 1968. Diurnal variation of Etesian winds in Athens. National Observatory of Athens. Publication No. 17 (in Greek).

Carapiperis LN. 1970. On the geographical distribution of the intensity of the Etesian winds in the Aegean Sea. National and Kapodistrian University, Athens.

Constatakopoulos KD. 1959. Problems of weather forecasting in Greece. Ph.D. thesis. National and Kapodistrian University, Athens (in Greek, abstract in English).

Dafis S. 2020. Contribution de la convection profonde à l'intensification des cyclones méditerranéens, Ph.D. thesis. Polytechnic Institute of Paris, Palaiseau (available in English).

Dafka S, Toreti A, Luterbacker J, Zanis P, Tyrlis E, Xoplaki E. 2018. On the ability of RCMs to capture the circulation patterns of Etesians. Climate Dynamics 51: 1687-1706. https://doi.org/10.1007/s00382-017-3977-2

Dandou A, Tombrou M, Kalogiros J, Bossioli E, Biskos G, Mihalopoulos N, Coe H. 2017. Investigation of turbulence parametrization schemes with reference to the atmospheric boundary layer over the Aegean Sea during etesian winds. Boundary-Layer Meteorology 164: 303-329. https://doi.org/10.1007/s10546-017-0255-0

Deutscher Wetterdienst. 2020. Operational and archived analyses. Available at: www.wetterzenntrale.de

Dudhia J. 1989. Numerical study of convection observed during the winter monsoon experiment using a mesoscale two-dimensional model. Journal of the Atmospheric Sciences 46: 3077-3107. https://doi.org/10.1175/1520-0469(1989)046%3C3077:NSOCOD%3E2.0.CO;2

Founda D, Tombrou M, Lalas DP, Asimakopoulos DN. 1997. Some measurements of turbulence characteristics over complex terrain. Boundary-Layer Meteorology 83: 221-245. https://doi.org/10.1023/A:1000288002105

Helmis CG, Asimakopoulos DN, Deligiorgi DG, Lalas DP. 1987. Observations of sea-breeze fronts near the shoreline. Boundary-Layer Meteorology 38: 395-410. https://doi.org/10.1007/BF00120854

Helmis CG, Kalogiros JA, Asimakopoulos DN, Papadopoulos KH, Soilemes AT. 1995. Acoustic sounder measurements of atmospheric turbulent fluxes on the shoreline. The Global Atmosphere and Ocean System 2: 351-362

Helmis CG, Jacovides C, Asimakopoulos DN, Flocas HA. 2002. Experimental study of the vertical structure of

the lower troposphere over a small Greek island in the Aegean Sea.

Journal of Atmospheric and Oceanic Technology 19: 1181-1192. https://doi.org/10.1175/1520-0426(2002)019<1181:ESOTVS>2.0.CO;2

Holton JR, Hakim GJ. 2013. An introduction to dynamic meteorology. Academic Press, Oxford, UK, 525 pp. https://doi.org/10.1016/B978-0-12-384866-6.00001-5

Hong GSY, Noah Y, Dudhia J. 2006. A new vertical diffusion package with an explicit treatment of entrainment processes. Monthly Weather Review 134: 2318-2341. https://doi.org/10.1175/MWR3199.1

Jiménez P, Dudhia J, González-Ruoco JF, Navarro J, Montavez JP, García-Bustamente E. 2012. A revised scheme for the WRF surface layer formulation. Monthly Weather Review 140: 898-918. https://doi.org/10.1175/MWR-D-11-00056.1

Kambezidis HD, Weidauer D, Melas D, Ulbricht M. 1998. Air quality in the Athens basin during sea breeze and non-sea breeze days using laser remote-sensing technique. Atmospheric Environment 32: 2173-2182. https://doi.org/10.1016/S1352-2310(97)00409-3

Kostopoulos VE, Helmis CG. 2014. Flux measurements in the surface marine atmospheric boundary layer over the Aegean Sea, Greece. Science of The Total Environment 494-495: 166-176. https://doi.org/10.1016/j.scitotenv.2014.06.127

Kotroni V, Lagouvardos K, Lalas D. 2001. The effect of the island of Crete on the Etesian winds over the Aegean Sea. Quarterly Journal of the Royal Meteorological Society 127: 1917-1937. https://doi.org/10.1002/qj.49712757604

Mariolopoulos EG, Mantis HT, Metaxas DA. 1981. Atmospheric boundary layer study the Aegean during the summer. Proceedings of the Academy of Athens 56 (in Greek, abstract in English).

Mavropoulou AM, Mantziafou A, Jarosz E, Sofianos S. 2016. The influence of Black Sea water inflow and its synoptic time-scale variability in the North Aegean Sea hydrodynamics. Ocean Dynamics 66: 195-206. https://doi.org/10.1007/s10236-016-0923-5

Melas D, Ziomas IC, Zerefos CH. 1995. Boundary layer dynamics in an urban coastal environment under sea breeze conditions. Atmospheric Environment 29: 3605-3617. https://doi.org/10.1016/1352-2310(95)00140-T

Melas D, Ziomas IC, Klemm O, Zerefos CH. 1998a. Flow dynamics in Athens area under moderate large-scale winds. Atmospheric Environment 32: 2209-2222. https://doi.org/10.1016/S1352-2310(97)00436-6

Melas D, Ziomas IC, Klemm O, Zerefos CH. 1998b. Anatomy of sea breeze circulation in Athens area under weak large-scale ambient winds. Atmospheric Environment 32: 2223-2237. https://doi.org/10.1016/s1352-2310(97)00420-2

Metaxas DA. 1970. A contribution to the study of the Etesian winds. Presented at the Mediterranean Meteorological Conference, under the auspices of USA Navy Weather Research Facility, Norfolk, Virginia.

Metaxas DA, Bartzokas A. 1994. Pressure covariability over the Atlantic, Europe and N. Africa. application: Centers of action for temperature, winter precipitation and summer winds in Athens, Greece. Theoretical and Applied Climatology 49: 9-18. https://doi.org/10.1007/BF00866284

Methymaki G, Bossioli E, Kalogiros J, Kouvarakis G, Mihalopoulos N, Nenes A, Tombrou M. 2020. Aerosol absorption over the Aegean Sea under northern summer winds. Atmospheric Environment 231: https://doi.org/10.1016/j.atmosenv.2020.117533

Mlawer EJ, Taubman SJ, Brown PD, Iacono MJ, Clough SA. 1997. Radiative transfer for inhomogeneous atmospheres: RRTM, a validated correlated-k model for the longwave. Journal of Geophysical Research 102: 16663-16682. https://doi.org/10.1029/97JD00237

Monin AS, Obukhov M. 1954. 'Osnovnye zakonomernosti turbulentnogo peremeshivanijav prizemnom sloe atmosfery Trudy geofiz. Inst. AN SSSR 24: 163-187. (Basic laws of turbulent mixing in the atmosphere near the ground. Contrib. Geophys. Inst. Acad. Sci. USSR 24: 163-187).

Owens RG, Hewson TD. 2018. ECMWF forecast user guide. Reading, UK, 112 pp. https://doi.org/10.21957/m1cs7h

Papanastasiou DK, Melas D. 2009. Climatology and impact on air quality of sea breeze in an urban coastal environment. International Journal of Climatology 29: 305-315. https://doi.org/10.1002/joc.1707

Papanastasiou DK, Melas D, Lissaridis I. 2010. Study of wind field under sea breeze and conditions: An application of WRF model. Atmospheric Research 98: 102-117. https://doi.org/10.1016/j.atmosres.2010.06.005

Pikros C. 1976. Sailplane and meteorology. Bulletin of the Hellenic Meteorological Society 1: 28-38.

Pikros C. 2000. Sea and mountain breezes in Greece.

Available at: http://www.marinaalimos.gr/smb

Pikros C, Prezerakos NG. 2006. Gathering information on the sea and mountain breezes characteristics in Peloponnesus, Greece. Proceedings of COMECAP vol. c, 241-249. Athens, Greece.

Prezerakos NG. 1975. Linear correlation of north component winds of ≥ 5 Beaufort force and the pressure difference between Thessaloniki (Mikra) and Rodhos. Meteorologica 51, University of Thessaloniki, 36 pp.

Prezerakos NG. 1985. Contribution of the wind field to genesis and evolution of barometric systems. Hellenic National Meteorological Service, Athens, 45 pp (in Greek, abstract in English).

Prezerakos NG. 1986. Characteristics of the sea breeze in Attica, Greece. Boundary-Layer Meteorology 36: 245-266. https://doi.org/10.1007/BF00118663

Prezerakos NG, Pikros C. 1989. The sea breeze front in Athens. Aeroathetics 19: 2-5.

Prezerakos NG, Flocas HA. 2002. Regional and global large-scale dynamics associated with a prolonged drought event in Greece. Journal of Atmospheric and Solar-terrestrial Physics 64: 1841-1854. https://doi.org/10.1016/S1364-6826(02)00197-9

Prezerakos NG, Nastos P, Mylonas S. 2018. Dynamics of the diurnal variation of the Etesian winds over Aegean Sea. Proceedings COMECAP 2018, October 15-17, Alexandroupolis, Greece, 183-195.

Prezerakos NG. 2022. Etesian winds outbursts over the Greek Seas and their linkage with larger-scale atmospheric circulation features: Two real time data case studies. Atmósfera 53: 89-110. https://doi.org/10.20937/ATM.52838

Repapis CC, Mantis EG. 1980. A type like land-sea breeze circulation as concluded from the diurnal waving of the barometric pressure over the Aegean Sea in summer. Meteorologica 69: 283-293.

Repapis CC, Zerefos CS, Tritakis B. 1977. On the Etesians over the Aegean. Proceedings of the Academy of Athens 52: 572-606.

Sahsamanoglou CS. 1976. The Sea breeze in Thessaloniki. Bulletin of the Hellenic Meteorological Society 1: 19-33 (in Greek, abstract in English).

Sandu I, Haiden T, Balsamo G, Schmederer, P, Arduini G, Day J, Beljaars A, Ben-Bouallegue Z, Boussetta S, Leutbecher M, Magnusson L, Rosnay P. 2020. Addressing near-surface forecast biases: Outcomes of the ECMWF project "Understanding uncertainties in surface-atmosphere" (USURF). ECMWF Technical Memo 875, Reading, UK, 43 pp. Available at: http://www.ecmwf.int/en/publications

Skamarock W, Klemp JB, Dudhia J, Gill DO, Liu Z, Berner J, et al. 2019. A Description of the Advanced Research WRF Model Version 4 (No. NCAR/TN-556+STR). Available at: https://doi.org/10.5065/1dfh-6p97

Soilemes AT, Helmis CG, Papageorgas PG, Asimakopoulos DN. 1993. A tethered balloon profiler system. Measurement Science and Technology 4: 1163-1168. https://doi.org/10.1088/0957-0233/4/10/022

Steyn DG, Kallos GA. 1992. A study of the dynamics of hodograph rotation in the sea breezes of Attika, Greece. Boundary-Layer Meteorology 58, 212-228. https://doi.org/10.1007/BF02033825

Stull RB. 1988. An introduction to boundary layer meteorology. Kluwer Academic Publishers. Dordrecht/Boston/London 670 pp. https://doi.org/10.1007/978-94-009-3027-8

Tombrou M, Dandou A, Helmis CG, Akylas E, Aggelopoulos G, Flocas H, Assimakopoulos VD, Soulakellis N. 2007. Model evaluation of the atmospheric boundary layer and mixed-layer evolution. Boundary-Layer Meteorology 124: 61-79. https://doi.org/10.1007/s10546-006-9146-5

Tombrou M, Bossioli E, Kalogiros J, Allan J, Bacak A, Biskos G, Coe H, Dandou A, Kouvarakis G, Mihalopoulos N, Percival CJ, Protonotariou AP, Szabó-Takács B. 2015. Physical and chemical processes of air masses in the Aegean Sea during Etesians: Aegean-game airborne campaign. Science of The Total Environment 506-507: 201-216. https://doi.org/10.1016/j.scitotenv.2014.10.098

Tyrlis E, Lelieveld J. 2013. Climatology and dynamics of the summer Etesian winds over the Eastern Mediterranean. Journal of the Atmospheric Sciences 70: 3374-3396. https://doi.org/10.1175/JAS-D-13-035.1

Van de Wiel BJH, Moene AF, Steeneveld GJ, Baas P, Bosveld FC, Holtslag AAM. 2010. A conceptual view on inertial oscillations and nocturnal low-level jets. Journal of the Atmospheric Sciences 67: 2679-2689. https://doi.org/10.1175/2010JAS3289.1

Varvayianni M, Helmis CG, Amanatidis GT, Asimakopoulos DN, Bartzis JG, Soilemes AT, Papadopoulos KH, Kambezidis H.D. 1993a. Effects of onshore topography on the sea breeze circulation. Pure and Applied Geophysics 140, 681-720. https://doi.org/10.1007/BF00876584

Varvayianni M., Bartzis JG, Helmis CG, Asimakopoulos DN. (1993b). Simulation of the sea breeze under

opposing synoptic conditions. Environmental Software 8, 19-27 https://doi.org/10.1016/0266-9838(93)90005-3

Wiin-Nielsen A. 1973. Dynamic meteorology. WMO-364. World Meteorological Organization, Geneva, 367 pp. Available at: https://library.wmo.int/?lvl=notice_display&id=7093#main

Zambakas JD. 973. The diurnal variation and duration of the sea breeze at the National Observatory of Athens, Greece. The Meteorological Magazine 102: 224-228. Available at: https://digital.nmla.metoffice.gov.uk/download/file/digitalFile_f5747485-96e3-4103-a43f-e5e7fff6cd55